Applying Janak's Theorem and Orbital Mixing to ZPL Estimations: The Case of the Negatively Charged Calcium Vacancy in Monolayer SiS_2

Rodrick Kuate Defo,[1,2] Haimi Nguyen,[3] Trevor D. Rhone,[4] Mark J. H. Ku,[5] and Georgios A. Tritsaris[2]

[1]*Department of Electrical Engineering, Princeton University, Princeton, NJ 08540*

[2]*John A. Paulson School of Engineering and Applied Sciences, Harvard University, Cambridge, MA 02138*

[3]*Department of Chemistry, Columbia University, New York, NY 10027*

[4]*Department of Physics, Applied Physics and Astronomy, Rensselaer Polytechnic Institute, Troy, NY 12180*

[5]*Department of Physics and Astronomy and Department of Materials Science and Engineering, University of Delaware, Newark, DE 19716*

(Dated: February 9, 2021)

Abstract

Since the observation of room-temperature, polarized and ultrabright single-photon emission from two-dimensional (2D) hexagonal boron nitride, much work has been done further investigating point defects in 2D materials. In order to identify the point defects, knowledge of the zero-phonon line (ZPL) is necessary. In this work, we present two new methods for rapid estimation of the ZPL. First, this ZPL is calculated in the hole picture by exploiting Janak's theorem, encouraged by the accuracy of the approach when applied to silicon monovacancies in $4H$-SiC. We provide a lowest order estimate of the error associated with using the theorem since the theorem is not exact for finite changes in occupation. The computation of this error is more rapid than the standard ΔSCF calculation. Next, we also show that initializing the charge density by mixing the ground state HOMO and LUMO can lead to faster convergence of an excited state self-consistent field (SCF) calculation compared to when the charge density is initialized from a superposition of atomic charges. We illustrate these methods using the case of the new singly negatively charged calcium vacancy in SiS_2, which we predict should exhibit inversion symmetry and which we propose as a qubit candidate.

I. INTRODUCTION

Research in the field of layered materials has grown quickly since the development of the high-quality sample yielding scotch-tape exfoliation technique [1, 2]. Such layered systems have allowed the observation of the quantum spin Hall effect at up to 100 K in monolayer tungsten ditelluride (WTe_2) [3] and the observation of a correlated insulator state by tuning the twist degree of freedom in bilayer structures of graphene, due to the presence of flat bands near zero Fermi energy at a twist angle of about 1.1°, which upon electrostatic doping yields superconducting states with a critical temperature of up to 1.7 K [4, 5]. Research in the field of point defect qubit candidates has also grown rapidly, particularly since the detection of single negatively charged nitrogen vacancy (NV^-) color centers in diamond [6]. These qubit candidates consist of impurities involving some small number of atoms and/or vacancies and act as single photon sources with indistinguishability of photons or negligible spectral diffusion being a desirable characteristic. Ensuing results include the room temperature coherent control of defect spin qubits in silicon carbide (SiC) [7], the discovery of the spectral stability of the germanium vacancy (GeV) in diamond [8], the optical spin polarization of the neutral silicon vacancy (SiV^0) in diamond [9] and the realization of spin coherence enhancement of a diamond spin qubit through strain tuning [10].

The layered material hexagonal boron nitride (h-BN) is of particular interest among layered materials as it has a wide bandgap [11], enabling it to encapsulate other layered materials and to host a variety of point defects giving rise to optical transitions lying within the range of its bandgap [2, 12–15]. The issue with h-BN as a host for a qubit candidate employing electronic spins is that the atomic nuclei of boron and nitrogen have spins as well, which can cause spin-decoherence of the electronic spin state. Such an argument invites consideration of SiS_2 as a host, which theory has predicted to exist in layered form between 2.8 GPa and 3.5 GPa for the space group $P2_1/c$ [16]. The SiS_2 host would be diamond-like or silicon carbide (SiC)-like in that the atoms that constitute it have a low natural abundance of isotopes with nuclear spin, which can be further suppressed via isotope purification in growth, diamond and SiC being systems that have been extensively studied as hosts for qubit candidates [7–10, 17–30]. The point defect we will investigate in SiS_2 has the further advantage of exhibiting inversion symmetry, which obviates the issue of an electric dipole moment making it susceptible to external noise and local fields and thus causing broadening of transitions. In identifying point defects in experiments, knowledge of the zero-phonon line (ZPL) transition is essential. We present in this paper a new method for estimating the error associated with computing the energy of the zero-phonon line (ZPL) transition of a point defect using Janak's theorem and a

new method for rapid convergence of excited state self-consistent field (SCF) calculations by mixing the HOMO and LUMO of a ground state calculation to initialize the charge density.

Janak's theorem states that [31],

$$\frac{\partial E}{\partial n_i} = \epsilon_i, \tag{1}$$

where E is the total energy, n_i is the orbital occupation of the i^{th} orbital, and ϵ_i is the corresponding eigenvalue of the orbital. This theorem is similar to Koopmans' theorem for Hartree-Fock theory [32] in that it relates energy differences under a change in the number of electrons to orbital energies. The theorem is in fact a density-functional theory (DFT) version of a theorem originally proved by Slater for his $X-\alpha$ method, which was introduced in an early attempt to account for both exchange and correlation in electronic structure calculations [33, 34]. As Janak's theorem does not imply that $\Delta E = \epsilon_i \Delta n_i$ for finite Δn_i, an estimate of the error associated with using the theorem to determine excitation energies where orbital occupations change by integer amounts is necessary. Applying the theorem and the method of error estimation is inherently faster than computing the energy of the excited state for a given point defect, as the error calculation amounts to terminating the excited state calculation before full convergence. We also show that excited state calculations for stable structures converge faster if the charge density is initialized by appropriately mixing the HOMO and LUMO from the ground state calculation, leaving the contribution to the charge density from the remaining orbitals unchanged, as compared to initialization of the charge density from a superposition of atomic charges.

In this work, we first outline the computational methods in Section II. We include in Section III the important results related to ZPL estimations for silicon monovacancies in 4H-SiC (see Section III A) and for the singly negatively charged calcium vacancy in SiS_2 (see Section III B, which also includes stability calculations) and a discussion of these results, ending with a summary of our conclusions.

II. THEORETICAL FORMULATION AND APPROACH

A. Calculation Method

The purpose of this work is to extend the notion of a mixing parameter [35] to the initialization of the charge density and to bolster the validity of using Janak's theorem [31] to calculate the zero-phonon line (ZPL) by demonstrating success for the case the singly negatively charged calcium vacancy in SiS_2, which we investigate as a potential qubit candidate. Indeed, the use of the Janak's theorem to calculate electronic properties of excited states of atoms, molecules, and solids, is not

novel [36, 37], but we additionally provide a lowest order estimate of the error associated with using the theorem for integral change in the occupation of the single particle states. To briefly overview the standard constrained-occupation DFT or ΔSCF method [38], the ground state scheme is applied to both the ground state and the lowest excited state by first filling up the lowest lying energy levels and calculating the energy of the resulting system and then constraining the occupation of the highest of these occupied levels to be zero and the lowest of the unoccupied levels to be one and again calculating the energy of the system. The energy difference is then taken as the energy of excitation, hence the term ΔSCF as the method is based on the energy difference between two self-consistent-field (SCF) calculations. We argue that the calculations in excess of the first ground state calculation are not always necessary, which directly follows from Janak's theorem in the limit where the change in occupation is infinitesimal. To motivate the argument, we compute the error between the ΔSCF approach and the approach of using Janak's theorem to lowest order under a change in occupation.

We consider the operator from the single particle equations in DFT,

$$\mathcal{O}(n(\mathbf{r})) = -\frac{\hbar^2}{2m_e}\nabla^2_{\mathbf{r}} + V(\mathbf{r}) + e^2\int \frac{n(\mathbf{r}')}{|\mathbf{r}-\mathbf{r}'|}\mathrm{d}\mathbf{r}' + \frac{\delta E_{\mathrm{xc}}[n(\mathbf{r})]}{\delta n(\mathbf{r}')}, \tag{2}$$

where $n(\mathbf{r})$ is the particle number density, the first term represents the kinetic energy of noninteracting quasiparticles with electron mass, the second term represents the external potential, the third term represents the Hartree potential for the Coulomb interaction between the quasiparticles and the last term represents the exchange-correlation potential recapturing the fermionic and many-body nature of electronic interactions. The single particle equation for the single particle state $\phi_i^{(n)}$ with eigenvalue $\epsilon_i^{(n)}$ then reads,

$$\mathcal{O}(n(\mathbf{r}))\phi_i^{(n)} = \epsilon_i^{(n)}\phi_i^{(n)}, \tag{3}$$

Under a change in occupation, let $n'(\mathbf{r})$ be the new number density and let $\phi_i^{(n')}$ be the new i^{th} single particle state such that,

$$\mathcal{O}(n'(\mathbf{r}))\phi_i^{(n')} = \epsilon_i^{(n')}\phi_i^{(n')}, \tag{4}$$

is satisfied. The equation for the total energy from DFT is [39],

$$E = \sum_i^N \epsilon_i^{(n)} - \frac{1}{2}\int\int \frac{n(\mathbf{r})n(\mathbf{r}')}{|\mathbf{r}-\mathbf{r}'|}\mathrm{d}\mathbf{r}\mathrm{d}\mathbf{r}' + \int n(\mathbf{r})\left[\epsilon_{\mathrm{xc}}(n(\mathbf{r})) - \mu_{\mathrm{xc}}(n(\mathbf{r}))\right]d\mathbf{r}. \tag{5}$$

If we let,

$$F(n(\mathbf{r})) = -\frac{1}{2}\int\int \frac{n(\mathbf{r})n(\mathbf{r}')}{|\mathbf{r}-\mathbf{r}'|}\mathrm{d}\mathbf{r}\mathrm{d}\mathbf{r}' + \int n(\mathbf{r})\left[\epsilon_{\mathrm{xc}}(n(\mathbf{r})) - \mu_{\mathrm{xc}}(n(\mathbf{r}))\right]d\mathbf{r}, \tag{6}$$

and

$$\Delta\epsilon = \sum_{i=1}^{N+1}(\epsilon_i^{(n')} - \epsilon_i^{(n)}) - (\epsilon_N^{(n')} - \epsilon_N^{(n)}) \tag{7}$$

then we can approximate the ΔSCF result as,

$$E_{\Delta\mathrm{SCF}} \approx \epsilon_{N+1}^{(n)} - \epsilon_N^{(n)} + \Delta\epsilon + F(n'(\mathbf{r})) - F(n(\mathbf{r})). \tag{8}$$

Therefore, if we only take the difference in ground state eigenvalues, the associated error is,

$$\Delta E_{\Delta\mathrm{SCF}} \approx \Delta\epsilon + F(n'(\mathbf{r})) - F(n(\mathbf{r})). \tag{9}$$

We can choose to obtain $n'(\mathbf{r})$ at any arbitrary iteration in the full constrained-occupation calculation for the excited state. Therefore, in the limit where $n'(\mathbf{r})$ is obtained at the final iteration of the full constrained-occupation calculation for the excited state, the error becomes exact. In performing the full constrained-occupation calculation for the excited state, we have also explored initializing the charge density by mixing the HOMO and LUMO by varying amounts.

B. Formation Energies

The formation energies of the calcium vacancy in SiS_2 in various charge states were calculated according to the formula [40, 41],

$$E_f(q) = E_{\mathrm{def}}(q) - E_0 - \sum_i \mu_i n_i + q(E_{\mathrm{VBM}} + E_{\mathrm{F}}) + E_{\mathrm{corr}}(q) \tag{10}$$

where q denotes the charge state, $E_{\mathrm{def}}(q)$ is the total energy for the defect supercell with charge state q, E_0 is the total energy for the stoichiometric neutral supercell, μ_i is the chemical potential of atom i, n_i is a positive (negative) integer representing the number of atoms added (removed) from the system relative to the stoichiometric cell, E_{VBM} is the absolute position of the valence band maximum, E_{F} is the position of the Fermi level with respect to the valence band maximum (generally treated as a parameter), and $E_{\mathrm{corr}}(q)$ is a correction term to account for the finite size of the supercell when performing calculations for charged defects [42]. This correction term does not simply treat the charged defect as a point charge, but rather considers the extended charge

distribution. The chemical potentials of all the reference elements used in our calculations are listed as follows as a function of their crystal structure and total energy per atom: Si (diamond structure, −5.42 eV/atom); S (the total energy of a gas phase S_8 molecule was calculated and the sublimation enthalpy was then subtracted [43, 44], −4.20 eV/atom); and Ca (face-centered cubic structure, −2.00 eV/atom). Consideration of Si-rich or S-rich preparation conditions was made, similar to previous work [29].

C. Material Screening Approach & Calculation Details

In order to leverage the vast body of existing knowledge in the field, we utilized an electronic database of two-dimensional materials called 2D Materials Encyclopedia [45] in a top-down filtering approach to find the most promising host materials. The entries from the database were first selected based on the presence of centrosymmetry in their space groups or of a horizontal mirror plane. The following filters were then applied,

1. *Band gap above 2 eV.* The optical transitions of the qubit candidate implanted in the host must not introduce interference from the electronic states of the host [22]. The value is taken to be at least as large as the energy of the optical transitions of well-known point defects such as the NV^- center in diamond and singly negatively charged silicon monovacancies in 4*H*-SiC.

2. *Exfoliation energy below 80 meV/atom.* The material must be easy to exfoliate and therefore to fabricate. The value is taken to be commensurate with exfoliation energies of common layered materials such as MoS_2 with space group $P\bar{6}m2$.

3. *Does not contain an atom with a nuclear spin.* Decoherence caused by the interaction of nuclear spins with the electronic ones of the qubit candidate must be minimized. We set the cutoff at $< 5\%$ natural abundance of isotopes containing a nuclear spin using as reference 4*H*-SiC.

The filtering process yielded SiS_2 and CaO as the only viable candidates and CaO is unstable.

Working from the literature on defects in diamond and 4*H*-SiC, we investigated vacancies, germanium-vacancy complexes and lead-vacancy complexes as possible qubit candidates in the SiS_2 host. However, these all break inversion symmetry when they are relaxed with spin polarization. On the other hand, the singly negatively charged calcium-vacancy complex is able to preserve inversion symmetry upon relaxation with spin polarization, due in part to the large size of the calcium atom.

To obtain the defect levels and total energies, we performed first-principles DFT calculations for the various defects in 4*H*-SiC and SiS_2 using the VASP code [46–48] and the QUANTUM

ESPRESSO code [49, 50] for ΔSCF calculations. In VASP, atomic structures were first converged using the generalized gradient approximation (GGA) for the exchange-correlation energy of electrons, as parametrized by Perdew, Burke and Erzenhof (PBE) [51] and then, for the calculation of defect levels, using the screened hybrid functional of Heyd, Scuseria and Ernzerhof (HSE) with the original parameters (0.2 $Å^{-1}$ for screening and 25% for mixing) [52, 53]. The atomic positions were relaxed until the magnitude of the Hellmann-Feynman forces was smaller than 10^{-4} eV·$Å^{-1}$ on each atom without spin-polarization and subsequently until the magnitude of the Hellmann-Feynman forces was smaller than 10^{-2} eV·$Å^{-1}$ on each atom with spin polarization to obtain defect levels and, for the stoichiometric conventional unit cell, the lattice parameters were concurrently relaxed. The wavefunctions were expanded in a plane wave basis with a cutoff energy of 500 eV for all systems and a Monkhorst-Pack grid of $6 \times 6 \times 2$ k-points was used for integrations in reciprocal space for SiS_2 and a Gamma centered grid of $4 \times 4 \times 2$ k-points was used for integrations in reciprocal space of 4H-SiC. The relaxed lattice parameters of the stoichiometric unit cell were then used for the supercell structures. Formation energies and defect levels were calculated using a supercell of 108 atoms for SiS_2 ($3 \times 3 \times 1$ multiple of the stoichiometric unit cell) with appropriately scaled k-point grids. For 4H-SiC, a supercell of 576 atoms ($6 \times 6 \times 2$ multiple of the stoichiometric unit cell) was used. The terms in $F(n(\mathbf{r}))$ were obtained for the ground state and for the state with the changed occupation, where a non-SCF calculation was performed until convergence keeping the charge density fixed in the latter case. The non-SCF calculation also provided the eigenvalues whose difference with the ground state eigenvalues we took. Code from work by Feenstra *et al.* [54] was used to change orbital occupations. In QUANTUM ESPRESSO, we performed ΔSCF calculations to investigate the SiS_2 system using PAW pseudopotentials [48] with a 108-atom supercell with gamma-point integration. Modified source code was used to alter the charge density in QUANTUM ESPRESSO.

III. RESULTS AND DISCUSSION

A. Silicon Monovacancies in 4H-SiC

We begin by demonstrating the accuracy of Janak's theorem for silicon monovacancies in 4H-SiC. For the lattice parameters of the stoichiometric hexagonal unit cell of 4H-SiC using the HSE06 functional, we find $a = 3.08$ Å and $c = 10.04$ Å. From the work of Soykal *et al.* [55], we know that for a spin-polarized system the approach of considering holes is equivalent to the approach of considering electrons. Defect levels calculated using the HSE06 functional for the singly negatively charged silicon monovacancy V_{Si}^{-} in 4H-SiC with $S = 3/2$ at the two inequiv-

alent h and k sites are illustrated schematically in Fig. 1 and are provided in Tables I and II. From the work of Soykal *et al.* [55], in the hole picture the ground state manifold is composed of the states, $||ue_xe_y + i\bar{u}\bar{e}_x\bar{e}_y\rangle/\sqrt{2}$, $||ue_xe_y - i\bar{u}\bar{e}_x\bar{e}_y\rangle/\sqrt{2}$, $||ue_x\bar{e}_y + u\bar{e}_xe_y + \bar{u}e_xe_y\rangle/\sqrt{3}$, $||\bar{u}\bar{e}_xe_y + \bar{u}e_x\bar{e}_y + u\bar{e}_x\bar{e}_y\rangle/\sqrt{3}$, while the excited state manifold in the hole picture is composed of the states, $||ve_xe_y + i\bar{v}\bar{e}_x\bar{e}_y\rangle/\sqrt{2}$, $||ve_xe_y - i\bar{v}\bar{e}_x\bar{e}_y\rangle/\sqrt{2}$, $||ve_x\bar{e}_y + v\bar{e}_xe_y + \bar{v}e_xe_y\rangle/\sqrt{3}$, $||\bar{v}\bar{e}_xe_y + \bar{v}e_x\bar{e}_y + v\bar{e}_x\bar{e}_y\rangle/\sqrt{3}$. Above, u and v are single particle orbitals transforming as the A_1 irreducible representation of the C_{3v} point group, while e_x and e_y transform as the x and y components of the two-dimensional E irreducible representation of the C_{3v} point group. The overbar denotes the minority spin state. To calculate the ZPL we take the lowest energy hole states, which from Tables I and II we see must be the $||\bar{u}\bar{e}_xe_y + \bar{u}e_x\bar{e}_y + u\bar{e}_x\bar{e}_y\rangle/\sqrt{3}$ (excited) and $||\bar{v}\bar{e}_xe_y + \bar{v}e_x\bar{e}_y + v\bar{e}_x\bar{e}_y\rangle/\sqrt{3}$ (ground) states. The ZPL we obtain for the k site V_{Si}^- is 1.34 eV, while the ZPL we obtain for the h site V_{Si}^- is 1.43 eV in excellent agreement with experimental values of 1.35 eV and 1.44 eV, respectively [56]. The slight underestimation of the ZPL values may therefore be due to the slightly smaller HSE06 band gap (3.18 eV compared to about 3.2 eV for experiment [57]). We note, however, that other theoretical calculations yield 1.44 eV for the k site and 1.54 eV for the h site using the HSE06 functional [58]. We believe error compensation in taking the difference of many eigenvalues may be causing the greater accuracy of our approximation to the ΔSCF method using Janak's theorem than the ΔSCF method itself, though later theoretical work shows better agreement with our work and with experiment [59].

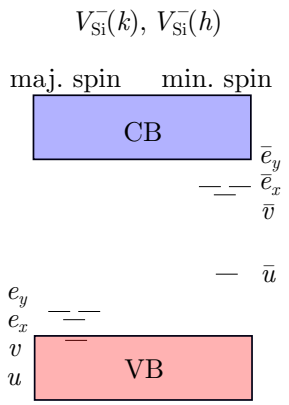

FIG. 1. Schematic of the majority (without overbar) and minority (with overbar) spin energy levels calculated in the ground state using the HSE06 functional for the $V_{\mathrm{Si}}^-(k)$ and $V_{\mathrm{Si}}^-(h)$ point defects in 4H-SiC. The conduction band is indicated in blue and the valence band in red. Single particle orbitals transforming as the A_1 irreducible representation of the C_{3v} point group are represented by u and v, while e_x and e_y transform as the x and y components of the two-dimensional E irreducible representation of the C_{3v} point group. The vertical axis of the figure is not drawn to scale.

TABLE I. DFT eigenvalues in eV calculated in the ground state using the HSE06 functional for the hole single particle states of the $V_{\mathrm{Si}}^{-}(k)$ point defect in 4H-SiC.

single particle state	majority spin	minority spin
u	7.553	8.116
v	7.773	10.011
e_x	7.828	10.152
e_y	7.855	10.225

TABLE II. DFT eigenvalues in eV calculated in the ground state using the HSE06 functional for the hole single particle states of the $V_{\mathrm{Si}}^{-}(h)$ point defect in 4H-SiC.

single particle state	majority spin	minority spin
u	7.551	8.119
v	7.800	10.137
e_x	7.871	10.227
e_y	7.906	10.289

Based on the results of the calculations for silicon monovacancies in 4H-SiC outlined above, Janak's theorem shows promise for rapid estimation of ZPL values. Indeed, we will see below that the accuracy of Janak's theorem is maintained for the most stable strain (ε) values of the singly negatively charged calcium vacancy in SiS_2 and that the error calculations we have outlined in Section II A provide a clear indication of when Janak's theorem fails.

B. Singly Negatively Charged Calcium Vacancy in SiS_2

As alluded to above, we now turn to demonstrating the continued accuracy of Janak's theorem for the two most stable ε values of the singly negatively charged calcium vacancy in SiS_2 and show that the associated error consistently identifies the larger discrepancies between the results of the theorem and the results of ΔSCF calculations. We also introduce results showing faster convergence of excited state SCF calculations when the charge density is initialized by mixing the HOMO and LUMO compared to when it is initialized from a superposition of atomic charges. For the lattice parameters of the stoichiometric unit cell SiS_2 with space group $P2_1/c$ using the PBE functional we find $a = 5.93$ Å, $b = 8.13$ Å, $\alpha = 90°$, $\beta = 102.57°$, $\gamma = 90°$ and a monolayer thickness of 3.65 Å with a vacuum of 16.94 Å. Using the HSE06 functional we find $a = 5.88$ Å, $b = 8.04$ Å, $\alpha = 90°$, $\beta = 103.11°$, $\gamma = 90°$ and a monolayer thickness of 3.59 Å with a vacuum of 16.67 Å. The approximation to the ZPL using Janak's theorem and using the ΔSCF method for different in-plane ε can be found in Fig. 2. We observe little variation of the approximation to the ZPL with tensile ε, but more variation with compressive ε which can also distort the structure. Since, due to Poisson's

ratio, the application of pressure should lead to tensile in-plane ε, we do not expect the ZPL value to change significantly from what we have predicted in experimentally realizable structures. The error calculations perform best for the uncompressed and $\varepsilon = +2\%$ structures, which have the smallest energy differences, obtaining the correct sign of the error as well, but fail to capture the correct sign and are much too large for the remaining ε values. The larger errors nonetheless correctly indicate more significant disagreement between the ΔSCF result and the result from using Janak's theorem. We note that based on a statistical learning based prediction of the bulk modulus [60, 61], the structures that should be the most stable given the requirement of an applied pressure of 2.8 GPa to 3.5 GPa are the uncompressed and $\varepsilon = +2\%$ structures, which is verified by QUANTUM ESPRESSO total energy calculations. As shown in Fig. 3, these most stable structures also responded best to performing the excited state calculation by replacing the initialization of the charge density from a superposition of atomic charges with the charge density of the ground state calculation, where the HOMO contribution is modified according to,

$$|\text{HOMO}\rangle \rightarrow \beta\,|\text{HOMO}\rangle + (1-\beta)\,|\text{LUMO}\rangle\,, \tag{11}$$

$0 \leq \beta \leq 1$. The value of the band-gap for the uncompressed structure using the PBE functional is 3.55 eV and the defect has total spin $S = 1/2$. The ΔSCF calculations and the differences in ground state eigenvalues were taken from QUANTUM ESPRESSO.

Based on the computational efficiency of our method for determining the error associated with using Janak's theorem demonstrated in Fig. 4, we argue that the approach of using Janak's theorem should be acceptable for screening large numbers of potential point defect single-photon emitter candidates for desired ZPL values. Our approach to the initialization of the charge density also shows promise for stable structures. A key point is that the search would focus on point defect candidates with total spin $S = 1/2$, otherwise more involved group theoretic arguments would be required to determine the correct many-body hole wavefunction as in the work of Soykal *et al.* [55]. The band-gap for the uncompressed structure using the HSE06 functional is 4.75 eV and we again find that the defect has total spin $S = 1/2$. Using QUANTUM ESPRESSO, the HSE06 calculation yields a ΔSCF result of 0.1705 eV and a difference in ground state eigenvalues of 0.2676 eV. Performing the error estimate outlined above yields an error of -0.0876 eV and took under 17 hours in VASP, while the constrained-occupation calculation for the excited state took over two days in QUANTUM ESPRESSO. The ΔSCF result for the HSE06 functional is close to the PBE results and we find in the literature that PBE results for energy differences can sometimes be as accurate as or more accurate

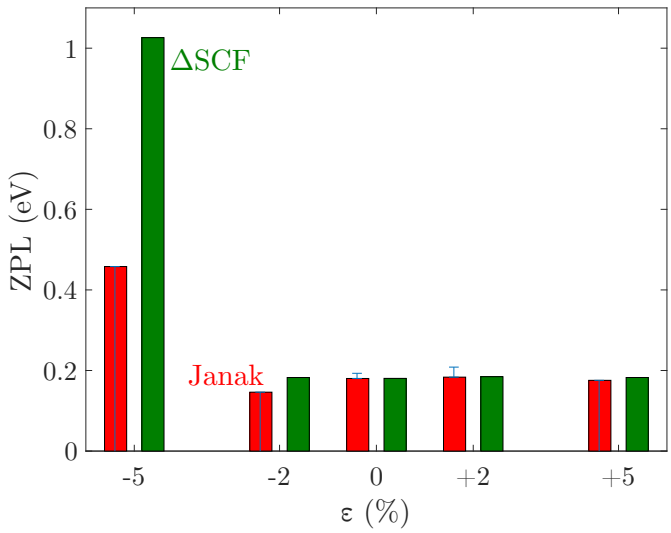

FIG. 2. ZPL values in eV, calculated using Janak's theorem (red) and using the ΔSCF method (green), for the singly negatively charged calcium vacancy in SiS_2 for in-plane $\varepsilon = \pm 2\%, \pm 5\%$ and for the uncompressed structure. The error associated with the result from Janak's theorem was calculated as described in Section II. The $\varepsilon = -5\%$ case caused the Ca atom to depart from the position that preserved inversion symmetry and was therefore not similar to the other structures.

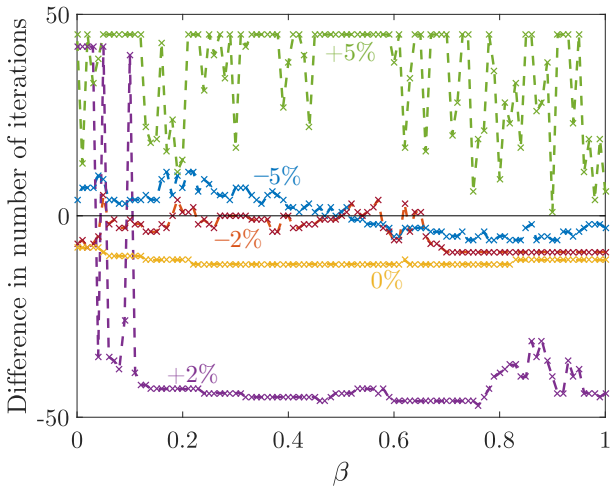

FIG. 3. Difference in the number of iterations to convergence between the initialization of the charge density obtained by changing the contribution of the HOMO to the ground state charge density according to Eq. (11) and the initialization of the charge density based on a superposition of atomic charges. In-plane $\varepsilon = \pm 2\%, \pm 5\%$ and the uncompressed structure were investigated. The maximum number of iterations was set at 100, which was attained for both $\varepsilon = +2\%$ and $\varepsilon = +5\%$ and explains the plateaus. We took $0 \leq \beta \leq 1$ and used increments of 0.01. Data points are indicated by '×' and the dashed lines are a guide for the eye.

than HSE06 ones for two-dimensional materials [62]. Therefore, modeling such materials within the framework of PBE where computational demands are smaller should suffice for a search.

The DFT partial charge densities obtained for ground hole (LUMO) and excited hole (HOMO)

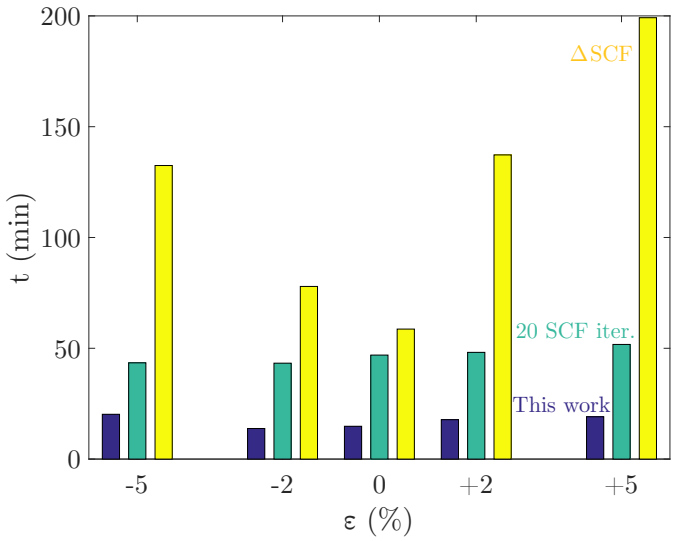

FIG. 4. Runtimes for convergence of the constrained-occupation calculation for the excited state (yellow), for completion of 20 SCF iterations (turquoise) and for calculation of the error associated wth using Janak's theorem using our method (blue). As our error calculations were done using the VASP code and the constrained-occupation calculations for the excited state were done using the QUANTUM ESPRESSO code, we took the time for a single SCF iteration for a given system from VASP and multiplied by the number of iterations required for the constrained-occupation calculation for the excited state in QUANTUM ESPRESSO to converge.

states and differences (LUMO − HOMO) are shown in Fig. 5. The differences show the closeness of certain LUMO-HOMO pairs. The structure of the defect is four missing atoms, two silicon and two sulfur, replaced by a single calcium atom such that the resulting point defect is inversion-symmetric, as confirmed by the partial charge densities in Fig. 5. This inversion symmetry is broken, however, for in-plane $\varepsilon = -5\%$. The lowest formation energy as a function of Fermi level is displayed in Fig. 6 for the uncompressed structure. The plot demonstrates that in sulfur-rich preparation conditions the introduction of a calcium vacancy actually stabilizes the SiS_2 structure with space group $P2_1/c$. Given the fact that the singly negatively charged calcium vacancy only exists for a very limited range of Fermi level values, it would be necessary to pin the Fermi level at the appropriate value either by doping the system or by gating as performed for example for graphene [4, 5]. Using a ^{43}Ca atom instead of a ^{40}Ca atom could also lead to coupling between the nuclear spin and the electronic spin to implement a long-lived quantum memory realized with the nuclear spin [63].

In sum, the case of the singly negatively charged calcium vacancy in SiS_2 confirms that using Janak's theorem and the associated error estimation for ZPL calculations is quick and clearly signals when the theorem is applicable. We have also shown that the full constrained occupation calculation for the excited state can be completed in some cases with fewer SCF iterations with careful initialization of the charge density.

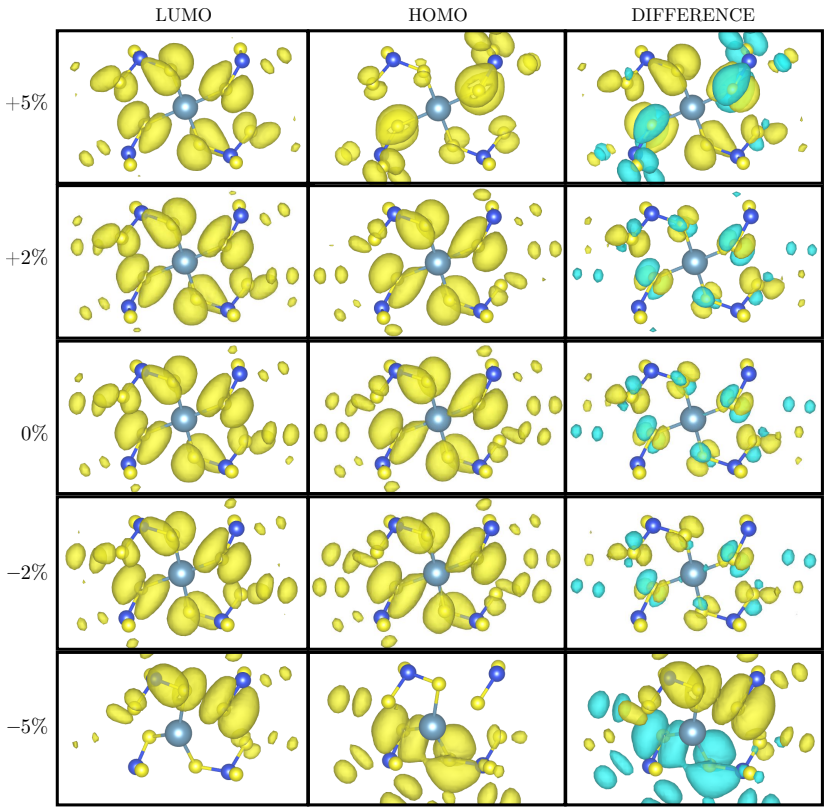

FIG. 5. DFT calculated partial charge densities for singly negatively charged calcium vacancy in SiS_2 for in-plane $\varepsilon = \pm 2\%, \pm 5\%$ and for the uncompressed structure are displayed corresponding to: the LUMO (left), the HOMO (middle) and the difference between the total charge densities with and without exchanging the occupations of the HOMO and LUMO (right). The value of ε is indicated to the left of the respective panels. Sulfur atoms are in yellow, silicon atoms are in blue and the calcium atom is in cyan. Charge accumulation (depletion) is indicated by translucent yellow (cyan). The isosurface of charge density is 0.0005 $e/\text{Å}^3$ for all plots.

IV. CONCLUSION

In conclusion, we propose the use of Janak's theorem for ZPL calculations and provide a quick new method for estimating the associated error. We also outline a new method for reducing the number of iterations required to converge excited state SCF calculations, compared to the default procedure for carrying out such calculations. Our ZPL results are consistent with previous experimental work where available and suggest that considering only ground state eigenvalues in the hole approach is a computationally efficient way of calculating optical excitation energies of color centers for screening purposes. Our novel method for initializing the charge density to reduce the number of iterations required for excited state calculations works well for stable structures. Finally, we propose the new singly negatively charged calcium vacancy in SiS_2, which has the advantage of being inversion-symmetric. The caveat is that it is not stable for most doping values, but we argue that doping or gating may help pin the Fermi level at the right value.

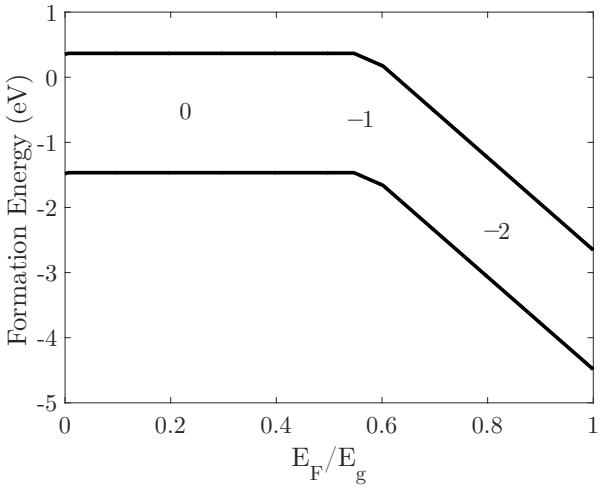

FIG. 6. Formation energy as a function of Fermi level for the calcium vacancy for a PBE DFT calculated gap $E_g = 3.55$ eV. The lower line corresponds to sulfur-rich preparation conditions while the upper line corresponds to silicon-rich preparation conditions. The integers between the lines indicate the most stable charge state of the defect at the corresponding values of the Fermi level. Calculations were done for the uncompressed structure.

ACKNOWLEDGMENTS: We thank Efthimios Kaxiras of Harvard University for useful discussions. We also acknowledge support by the STC Center for Integrated Quantum Materials, NSF Grant No. DMR-1231319. This work used computational resources of the Extreme Science and Engineering Discovery Environment (XSEDE), which is supported by National Science Foundation Grant Number ACI-1548562, [64] on Stampede2 at TACC through allocation TG-DMR120073, and of the National Energy Research Scientific Computing Center (NERSC), a U.S. Department of Energy Office of Science User Facility operated under Contract No. DE-AC02-05CH11231.

[1] A. K. Geim and I. V. Grigorieva, Nature **499**, 419 (2013).

[2] M. Toth and I. Aharonovich, Annual Review of Physical Chemistry **70**, 123 (2019).

[3] S. Wu, V. Fatemi, Q. D. Gibson, K. Watanabe, T. Taniguchi, R. J. Cava, and P. Jarillo-Herrero, Science **359**, 76 (2018).

[4] Y. Cao, V. Fatemi, A. Demir, S. Fang, S. L. Tomarken, J. Y. Luo, J. D. Sanchez-Yamagishi, K. Watanabe, T. Taniguchi, E. Kaxiras, R. C. Ashoori, and P. Jarillo-Herrero, Nature **556**, 80 (2018).

[5] Y. Cao, V. Fatemi, S. Fang, K. Watanabe, T. Taniguchi, E. Kaxiras, and P. Jarillo-Herrero, Nature **556**, 43 (2018).

[6] A. Gruber, A. Dräbenstedt, C. Tietz, L. Fleury, J. Wrachtrup, and C. v. Borczyskowski, Science **276**, 2012 (1997).

[7] W. F. Koehl, B. B. Buckley, F. J. Heremans, G. Calusine, and D. D. Awschalom, Nature **479**, 84 (2011).

[8] P. Siyushev, M. H. Metsch, A. Ijaz, J. M. Binder, M. K. Bhaskar, D. D. Sukachev, A. Sipahigil, R. E. Evans, C. T. Nguyen, M. D. Lukin, P. R. Hemmer, Y. N. Palyanov, I. N. Kupriyanov, Y. M. Borzdov, L. J. Rogers, and F. Jelezko, Phys. Rev. B **96**, 081201 (2017).

[9] B. L. Green, S. Mottishaw, B. G. Breeze, A. M. Edmonds, U. F. S. D'Haenens-Johansson, M. W. Doherty, S. D. Williams, D. J. Twitchen, and M. E. Newton, Phys. Rev. Lett. **119**, 096402 (2017).

[10] Y.-I. Sohn, S. Meesala, B. Pingault, H. A. Atikian, J. Holzgrafe, M. Gündoğan, C. Stavrakas, M. J. Stanley, A. Sipahigil, J. Choi, M. Zhang, J. L. Pacheco, J. Abraham, E. Bielejec, M. D. Lukin, M. Atatüre, and M. Lončar, Nat. Commun. **9**, 2012 (2018).

[11] C. Elias, P. Valvin, T. Pelini, A. Summerfield, C. J. Mellor, T. S. Cheng, L. Eaves, C. T. Foxon, P. H. Beton, S. V. Novikov, B. Gil, and G. Cassabois, Nature Communications **10**, 2639 (2019).

[12] T. T. Tran, K. Bray, M. J. Ford, M. Toth, and I. Aharonovich, Nature Nanotechnology **11**, 37 (2015).

[13] V. Ivády, G. Barcza, G. Thiering, S. Li, H. Hamdi, J.-P. Chou, Ö. Legeza, and A. Gali, npj Computational Materials **6**, 41 (2020).

[14] M. Abdi, J.-P. Chou, A. Gali, and M. B. Plenio, ACS Photonics **5**, 1967 (2018).

[15] A. Gottscholl, M. Kianinia, V. Soltamov, S. Orlinskii, G. Mamin, C. Bradac, C. Kasper, K. Krambrock, A. Sperlich, M. Toth, I. Aharonovich, and V. Dyakonov, Nature Materials **19**, 540 (2020).

[16] D. Plašienka, R. Martoňák, and E. Tosatti, Scientific Reports **6**, 37694 (2016).

[17] R. Kuate Defo, E. Kaxiras, and S. L. Richardson, Journal of Applied Physics **126**, 195103 (2019).

[18] J. N. Becker, B. Pingault, D. Groß, M. Gündoğan, N. Kukharchyk, M. Markham, A. Edmonds, M. Atatüre, P. Bushev, and C. Becher, Phys. Rev. Lett. **120**, 053603 (2018).

[19] M. W. Doherty, N. B. Manson, P. Delaney, F. Jelezko, J. Wrachtrup, and L. C. L. Hollenberg, Physics Reports **528**, 1 (2013), the nitrogen-vacancy colour centre in diamond.

[20] A. Gali, A. Gällström, N. Son, and E. Janzén, in *Silicon Carbide and Related Materials 2009*, Materials Science Forum (Trans Tech Publications Ltd, 2010) p. 395.

[21] S.-Y. Lee, M. Widmann, T. Rendler, M. W. Doherty, T. M. Babinec, S. Yang, M. Eyer, P. Siyushev, B. J. M. Hausmann, M. Loncar, Z. Bodrog, A. Gali, N. B. Manson, H. Fedder, and J. Wrachtrup, Nature Nanotechnology **8**, 487 (2013).

[22] J. R. Weber, W. F. Koehl, J. B. Varley, A. Janotti, B. B. Buckley, C. G. Van de Walle, and D. D. Awschalom, Proceedings of the National Academy of Sciences **107**, 8513 (2010).

[23] V. A. Soltamov, A. A. Soltamova, P. G. Baranov, and I. I. Proskuryakov, Phys. Rev. Lett. **108**, 226402 (2012).

[24] H. Kraus, V. A. Soltamov, D. Riedel, S. Väth, F. Fuchs, A. Sperlich, P. G. Baranov, V. Dyakonov, and G. V. Astakhov, Nature Physics **10**, 157 (2014).

[25] U. Wahl, J. G. Correia, R. Villarreal, E. Bourgeois, M. Gulka, M. Nesládek, A. Vantomme, and L. M. C. Pereira, Phys. Rev. Lett. **125**, 045301 (2020).

[26] J.-F. Wang, Q. Li, F.-F. Yan, H. Liu, G.-P. Guo, W.-P. Zhang, X. Zhou, L.-P. Guo, Z.-H. Lin, J.-M. Cui, X.-Y. Xu, J.-S. Xu, C.-F. Li, and G.-C. Guo, ACS Photonics **6**, 1736 (2019).

[27] W. Dong, M. W. Doherty, and S. E. Economou, Phys. Rev. B **99**, 184102 (2019).

[28] B. L. Green, M. W. Doherty, E. Nako, N. B. Manson, U. F. S. D'Haenens-Johansson, S. D. Williams, D. J. Twitchen, and M. E. Newton, Phys. Rev. B **99**, 161112 (2019).

[29] R. Kuate Defo, X. Zhang, D. Bracher, G. Kim, E. Hu, and E. Kaxiras, Phys. Rev. B **98**, 104103 (2018).

[30] R. Kuate Defo, R. Wang, and M. Manjunathaiah, Journal of Computational Science (2019).

[31] J. F. Janak, Phys. Rev. B **18**, 7165 (1978).

[32] T. Koopmans, Physica **1**, 104 (1934).

[33] J. C. Slater and J. H. Wood, International Journal of Quantum Chemistry **5**, 3 (1970).

[34] E. Kaxiras, *Atomic and Electronic Structure of Solids* (Cambridge University Press, New York, 2003).

[35] D. D. Johnson, Phys. Rev. B **38**, 12807 (1988).

[36] J. C. Slater, J. B. Mann, T. M. Wilson, and J. H. Wood, Phys. Rev. **184**, 672 (1969).

[37] N. Hadjisavvas and A. Theophilou, Phys. Rev. A **32**, 720 (1985).

[38] R. O. Jones and O. Gunnarsson, Rev. Mod. Phys. **61**, 689 (1989).

[39] W. Kohn and L. J. Sham, Phys. Rev. **140**, A1133 (1965).

[40] S. B. Zhang and J. E. Northrup, Phys. Rev. Lett. **67**, 2339 (1991).

[41] C. Freysoldt, B. Grabowski, T. Hickel, J. Neugebauer, G. Kresse, A. Janotti, and C. G. Van de Walle, Rev. Mod. Phys. **86**, 253 (2014).

[42] D. Vinichenko, M. G. Sensoy, C. M. Friend, and E. Kaxiras, Phys. Rev. B **95**, 235310 (2017).

[43] R. K. Defo, S. Fang, S. N. Shirodkar, G. A. Tritsaris, A. Dimoulas, and E. Kaxiras, Phys. Rev. B **94**, 155310 (2016).

[44] R. Steudel, *Elemental Sulfur and Sulfur-Rich Compounds I*.

[45] J. Zhou, L. Shen, M. D. Costa, K. A. Persson, S. P. Ong, P. Huck, Y. Lu, X. Ma, Y. Chen, H. Tang, and Y. P. Feng, Scientific Data **6**, 86 (2019), www.2DMatPedia.org.

[46] G. Kresse and J. Hafner, Phys. Rev. B **47**, 558 (1993).

[47] G. Kresse and J. Furthmüller, Phys. Rev. B **54**, 11169 (1996).

[48] G. Kresse and D. Joubert, Phys. Rev. B **59**, 1758 (1999).

[49] P. Giannozzi, S. Baroni, N. Bonini, M. Calandra, R. Car, C. Cavazzoni, D. Ceresoli, G. L. Chiarotti, M. Cococcioni, I. Dabo, A. D. Corso, S. de Gironcoli, S. Fabris, G. Fratesi, R. Gebauer, U. Gerstmann, C. Gougoussis, A. Kokalj, M. Lazzeri, L. Martin-Samos, N. Marzari, F. Mauri, R. Mazzarello, S. Paolini, A. Pasquarello, L. Paulatto, C. Sbraccia, S. Scandolo, G. Sclauzero, A. P. Seitsonen, A. Smogunov, P. Umari, and R. M. Wentzcovitch, Journal of Physics: Condensed Matter **21**, 395502 (2009).

[50] P. Giannozzi, O. Andreussi, T. Brumme, O. Bunau, M. B. Nardelli, M. Calandra, R. Car, C. Cavazzoni, D. Ceresoli, M. Cococcioni, N. Colonna, I. Carnimeo, A. D. Corso, S. de Gironcoli, P. Delugas, R. A. DiStasio, A. Ferretti, A. Floris, G. Fratesi, G. Fugallo, R. Gebauer, U. Gerstmann, F. Giustino, T. Gorni, J. Jia, M. Kawamura, H.-Y. Ko, A. Kokalj, E. Küçükbenli, M. Lazzeri, M. Marsili, N. Marzari, F. Mauri, N. L. Nguyen, H.-V. Nguyen, A. O. de-la Roza, L. Paulatto, S. Poncé, D. Rocca, R. Sabatini, B. Santra, M. Schlipf, A. P. Seitsonen, A. Smogunov, I. Timrov, T. Thonhauser, P. Umari, N. Vast, X. Wu, and S. Baroni, Journal of Physics: Condensed Matter **29**, 465901 (2017).

[51] J. P. Perdew, K. Burke, and M. Ernzerhof, Phys. Rev. Lett. **77**, 3865 (1996).

[52] J. Heyd, G. E. Scuseria, and M. Ernzerhof, The Journal of Chemical Physics **118**, 8207 (2003).

[53] A. V. Krukau, O. A. Vydrov, A. F. Izmaylov, and G. E. Scuseria, The Journal of Chemical Physics **125**, 224106 (2006).

[54] R. M. Feenstra, N. Srivastava, Q. Gao, M. Widom, B. Diaconescu, T. Ohta, G. L. Kellogg, J. T. Robinson, and I. V. Vlassiouk, Phys. Rev. B **87**, 041406 (2013).

[55] O. O. Soykal, P. Dev, and S. E. Economou, Phys. Rev. B **93**, 081207 (2016).

[56] D. O. Bracher, X. Zhang, and E. L. Hu, Proceedings of the National Academy of Sciences **114**, 4060 (2017).

[57] P. Paufler, Crystal Research and Technology **22**, 1158 (1987).

[58] V. Ivády, J. Davidsson, N. T. Son, T. Ohshima, I. A. Abrikosov, and A. Gali, Phys. Rev. B **96**, 161114 (2017).

[59] P. Udvarhelyi, G. m. H. Thiering, N. Morioka, C. Babin, F. Kaiser, D. Lukin, T. Ohshima, J. Ul-Hassan, N. T. Son, J. Vučković, J. Wrachtrup, and A. Gali, Phys. Rev. Applied **13**, 054017 (2020).

[60] M. de Jong, W. Chen, R. Notestine, K. Persson, G. Ceder, A. Jain, M. Asta, and A. Gamst, Scientific Reports **6**, 34256 (2016).

[61] J. Evers, P. Mayer, L. Moeckl, G. Oehlinger, R. Koeppe, and H. Schnoeckel, Inorganic Chemistry **54**, 1240 (2015).

[62] P. Johari and V. B. Shenoy, ACS Nano **6**, 5449 (2012), pMID: 22591011.

[63] M. Pfender, N. Aslam, H. Sumiya, S. Onoda, P. Neumann, J. Isoya, C. A. Meriles, and J. Wrachtrup, Nature Communications **8**, 834 (2017).

[64] J. Towns, T. Cockerill, M. Dahan, I. Foster, K. Gaither, A. Grimshaw, V. Hazlewood, S. Lathrop, D. Lifka, G. D. Peterson, R. Roskies, J. R. Scott, and N. Wilkins-Diehr, Computing in Science & Engineering **16**, 62 (2014).